Amplified Single Base-Pair Mismatch Detection via Aggregation of Exonuclease-Sheared Gold Nanoparticles

Shuo Wu,[†,‡] Pingping Liang,[†] Haixiang Yu,[†] Xiaowen Xu,[†] Yuan Liu,[†] Xinhui Lou,[§] and Yi Xiao*[,†]

[†]Department of Chemistry and Biochemistry, Florida International University, 11200 SW eighth Street, Miami, FL, 33199
[‡]Department of Chemistry, Dalian University of Technology, Linggong Rd. 2, Dalian, China, 116023
[§]Department of Chemistry, Capital Normal University, Xisanhuan North Rd. 105, Beijing, China, 100048

Ⓢ *Supporting Information*

ABSTRACT: Single nucleotide polymorphism (SNP) detection is important for early diagnosis, clinical prognostics, and disease prevention, and a rapid and sensitive low-cost SNP detection assay would be valuable for resource-limited clinical settings. We present a simple platform that enables sensitive, naked-eye detection of SNPs with minimal reagent and equipment requirements at room temperature within 15 min. SNP detection is performed in a single tube with one set of DNA probe-modified gold nanoparticles (AuNPs), a single exonuclease (Exo III), and the target in question. Exo III's apurinic endonucleolytic activity differentially processes hybrid duplexes between the AuNP-bound probe and DNA targets that are perfectly matched or contain a single-base mismatch.

For perfectly matched targets, Exo III's exonuclease activity facilitates a process of target recycling that rapidly shears DNA probes from the particles, generating an AuNP aggregation-induced color change, whereas no such change occurs for mismatched targets. This color change is easily observed with as little as 2 nM of target, 100-fold lower than the target concentration required for reliable naked eye observation with unmodified AuNPs in well-optimized reaction conditions. We further demonstrate that this system can effectively discriminate a range of different mismatches.
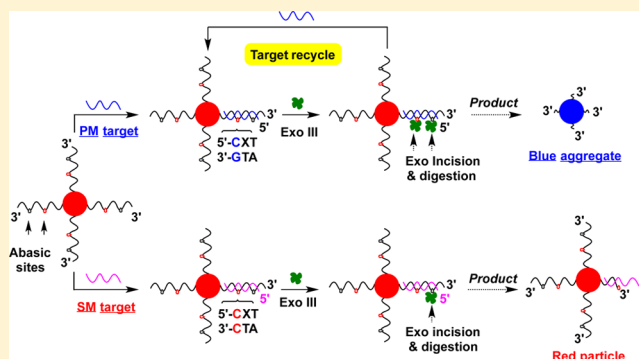
Ninety percent of human genetic variation takes the form of single nucleotide polymorphisms (SNPs), and these are involved in the etiology of many human diseases.[1] SNP detection is therefore important for early diagnosis, clinical prognostics, and disease prevention.[2,3] Accordingly, numerous enzyme-based SNP detection schemes have been developed, including microarray-based sequencing,[4,5] primer extension,[6] ligation-based methods,[7] enzyme invasive cleavage,[8] and TaqMan assays.[9] Although these methods can achieve parallel, sensitive detection of SNPs, they are complex, multistep techniques that require costly modified primers and are often plagued by issues related to enzymatic efficiency and product separation. Hybridization-based SNP detection methods such as dynamic allele-specific hybridization,[10] molecular beacons,[11] binary probes,[12] and triple-stem probes[13] offer an alternative for identifying specific target sequences. However, these suffer from low sensitivity or poor specificity at room temperature, and effective SNP discrimination usually requires the use of high-stringency conditions with precise temperature control. Additionally, the time, expense, and specialized equipment and trained personnel required for these various methods can make them impractical for use in small hospital or developing-world settings. As such, there remains an urgent need for a simple platform for rapid and sensitive SNP detection at room temperature.

Gold nanoparticles (AuNPs) are widely used for DNA sensing,[14] largely because of two important advantages. First, it is straightforward to achieve surface modification of AuNPs with hundreds of DNA probes.[15] Second, because the response of AuNPs to light is strongly dictated by their environment, size, and physical dimensions, one can readily tune the visible properties of AuNPs by changing their size, shape, surface chemistry, or aggregation state.[16] The resulting color change can be so great that it is readily visible to the eye. The Mirkin group was the first to report an AuNP-based SNP detection scheme, which relied on hybridization-driven changes in AuNP aggregation.[17] In this assay, two sets of DNA-modified AuNPs were cross-linked via target hybridization, and a single-base mismatch was directly observed on a C18 thin-layer chromatography plate at 58 °C.[17] To obtain clinically relevant sensitivity, however, this and subsequently developed AuNP-based SNP detection platforms have required the use of polymerase chain reaction,[18] nicking endonuclease,[19] rolling circle amplification,[20] or real-time ligation chain reaction[21] to amplify their target prior to detection. Low picomolar concentrations of target can be successfully detected using
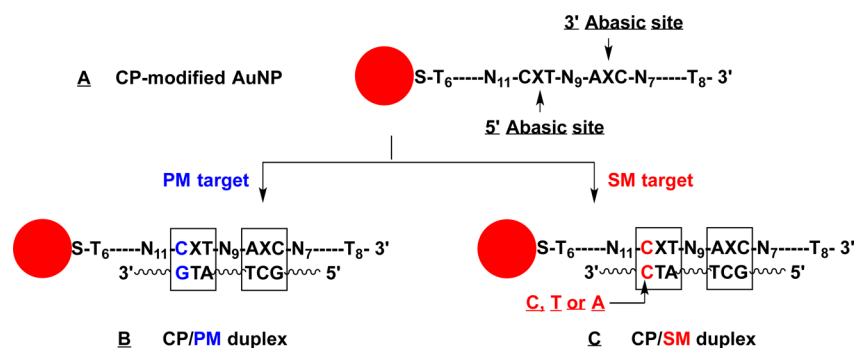
Figure 1. Scheme for CP-modified AuNP, CP/PM, and CP/SM duplexes. Each CP is conjugated to the gold nanoparticle via a thiol linkage to a flexible poly (T_6) linker at the probe's 5′ end (A). The 45-nt CP is designed to match the SNP-containing target sequence of interest and features two propanyl abasic sites (denoted by 'X'). The 5′ abasic site is situated at a position immediately 5′ to the SNP site. When a perfectly matched (PM) target DNA hybridizes with the CP, it forms a CP/PM duplex (B) in which both the 5′ and 3′ abasic sites are flanked by matched bases, which facilitates Exo III endonucleolytic incision. In contrast, the single-base mismatched (SM) duplex (CP/SM) contains a single C−C mismatch-adjacent to the 5′ abasic site (C), inhibiting Exo III endonucleolytic digestion.

these amplified approaches, but the target-triggered aggregation of AuNPs requires a reaction time of at least 2 h, with precise temperature control needed. An alternate approach uses the color change of unmodified AuNPs to identify SNPs.[22] This method is based on differences in electrostatic interaction between single- and double-stranded DNA on unmodified AuNPs.[22] Typically, the adsorption of single-stranded DNA stabilizes AuNPs against aggregation at salt concentrations that would ordinarily cause colloid aggregation. Thus, single-base mismatched targets could be detected through a red-to-blue color change within 5 min.[22] However, even for well-optimized reaction conditions, reliable detection with unmodified AuNPs required a target concentration ≥200 nM for naked eye observation.[23]

In response to the above limitations, we describe here a simple and rapid colorimetric platform that can conduct SNP detection in high-salt buffer without the need for specialized equipment or a complex temperature ramping program. Our platform employs an AuNP-based, exonuclease III (Exo III) amplified strategy to achieve colorimetric SNP detection at low nanomolar target concentrations. The detection is performed in a single tube with a single set of DNA capture probe (CP)-modified AuNPs (Figure 1A), Exo III, and target DNA. Exo III has been reported to have 3′-to-5′ exonuclease, RNase H, 3′-phosphatase, and apurinic endonuclease activities.[24] In this work, we take advantage of Exo III's apurinic endonucleolytic activity to distinguish between duplexes formed by CP probes with either perfectly matched (PM) or single-base mismatched (SM) DNA targets, after which we employ this enzyme's 3′-to-5′ exonuclease activity in a target-recycling mechanism that rapidly generates a visible color readout within 15 min. This enables unambiguous naked-eye identification of SNP genotypes at room temperature. If the target sequence is perfectly matched to the CP sequence on the AuNPs (Figure 1B, CP/PM duplex), the sensor undergoes Exo III-amplified AuNP aggregation that yields a blue color; in the case of a single-base mismatch (Figure 1C, CP/SM duplex), the sensor fails to aggregate and remains red. This is the first example to demonstrate an amplified, colorimetric SNP detection via a rapid aggregation of Exo III-sheared AuNPs at room temperature.

The preparation of our sensor begins with the synthesis of DNA CP-conjugated AuNPs. We first synthesized citrate-capped AuNPs (12 ± 1 nm diameter) as previously reported[25] and determined their concentration by measuring the maximum absorbance at 518 nm. We then attached our 5′

thiolated CP DNAs (CP, **1**, 45-nt) to the freshly prepared AuNPs. The probe features a 5′ and a 3′ propanyl abasic site and is designed as follows: 5′-thiol − poly(T_6) − $(N)_{11}$ − 5′ abasic site (5′-CXT) − $(N)_9$ − 3′ abasic site (AXC-3′) − $(N)_7$ − poly(T_8)-3′. The 5′ poly(T_6) acts as a flexible linker to improve target hybridization, and the 3′ poly(T_8) serves as a sticky end to protect the CP against exonucleolytic digestion by Exo III. This probe is specifically designed to recognize a target DNA sequence in which the SNP site is situated directly 5′ to the 5′ abasic site. The function of the 3′ abasic site is to fragment the probe in order to easily facilitate target release at room temperature.

The CP-modified AuNPs are homogeneously dispersed in high-salt reaction buffer (20 mM Tris-acetate (pH 7.9), 50 mM KAc, 25 mM NaCl, 3 mM Mg^{2+}, and 20 mM Ca^{2+}) due to protection by the immobilized CP strands (Figure 2A). Typically, the solution is red in color. In the absence of target, these immobilized CPs are resistant to the 3′-to-5′ exonucleolytic activity of Exo III by their single-stranded structure, and we did not observe any digestion within 2 h (Figure 3A,B, probe + control).

We then hybridized the modified AuNPs with either perfectly matched (PM, **2**, 33-nt) or single-base mismatched (SM, **3**, 33-nt) DNA targets. The PM target forms a duplex with the immobilized CP in which both the 5′ and 3′ abasic sites are flanked by matched bases, with the 3′ poly(T_8) sequence of CP forming a sticky end (Figure 2B). Exo III is inactive at this 3′ sticky end[26] and instead preferentially cleaves the match-flanked abasic sites through its apurinic endonucleolytic activity (Figure 2C), converting the CP into three nicked duplex fragments (12-, 11-, and 8-bp). Exo III then recognizes the newly formed 3′-hydroxyl termini on the nicked ends of the CP fragments and rapidly catalyzes the stepwise removal of 5′-mononucleotides through its exonucleolytic activity (Figure 2D). This shears the CP fragments from the particle but releases the PM strand intact (Figure 2E). The released PM target is then recycled and hybridizes with another CP on the same or a different AuNP to begin the cycle anew (Figure 2F). Ultimately, all of the 45-nt CPs are sheared from the AuNPs, leaving only short poly(T_6) linkers behind on the particles. The sheared AuNPs become unstable in the reaction buffer and undergo salt-induced aggregation (Figure 2G), giving rise to a red-to-blue color change (Figure 3, PM). Because a single target can be recycled for many CP-modified AuNPs, the
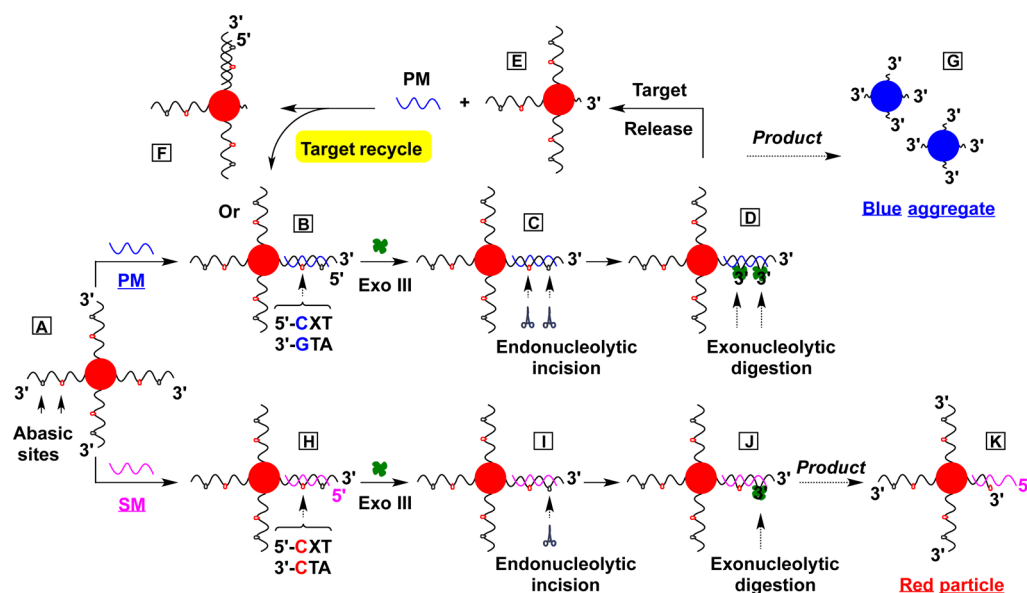
Figure 2. Scheme for AuNP-based, Exo III-amplified colorimetric SNP detection. (A) The CP-modified AuNPs are homogeneously dispersed in the buffer. (B) PM target hybridization with CP forms a perfectly matched duplex with a 3′ poly(T$_8$) sticky end. (C) Exo III preferentially cleaves both match-flanked abasic sites through its apurinic endonucleolytic activity, generating two nicks. (D) Exo III recognizes the 3′-hydroxyl termini on these nicked ends and rapidly digests these fragments via its exonucleolytic activity. (E) The CP fragments are sheared from the particle, releasing the intact PM target. (F) The PM target is recycled, hybridizing with a new CP on the same or a different AuNP. (G) In the absence of CP strands, the AuNPs undergo salt-induced aggregation with an associated red-to-blue color change. (H) In contrast, a single mismatch flanking the 5′ abasic site in the CP−SM duplex inhibits the apurinic endonucleolytic activity of Exo III. (I) Exo III therefore only cleaves the match-flanked 3′ abasic site, generating a single nick. (J) The enzyme subsequently performs 3′-to-5′ exonucleolytic digestion. (K) DNA digestion dramatically slows down as Exo III approaches the mismatch-flanked 5′ abasic site, leaving behind DNA duplex fragments on the particle. These fragments prevent salt-induced AuNP aggregation, and the solution remains red.
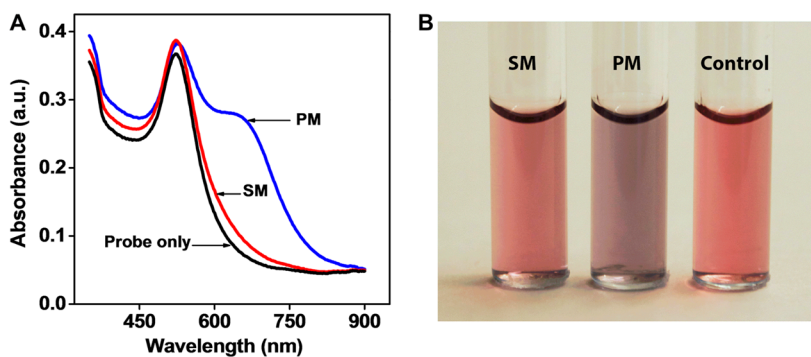

Figure 3. Our sensor achieves colorimetric SNP detection within 15 min at room temperature. (A) UV−vis spectra of reactions performed in the presence of 50 U Exo III with CP-modified AuNPs alone (probe only) or with 20 nM SM or PM. (B) A red-to-blue color change is apparent in the PM sample relative to the SM sample or probe only (control).

SNP signal is rapidly amplified with visible AuNP aggregation within 15 min.

In contrast, the CP-SM duplex contains a single C−C mismatch-flanked 5′ abasic site (5′-CXT/CTA) (Figure 2H), which significantly inhibits the apurinic endonucleolytic activity of Exo III.[27] Exo III therefore preferentially only cleaves the match-flanked 3′ abasic site, generating two nicked CP duplex fragments (23- and 8-bp) (Figure 2I). The enzyme subsequently catalyzes exonucleolytic digestion at this site (Figure 2J). However, this digestion dramatically slows down as Exo III approaches the uncleaved mismatch-flanked 5′ abasic site,[28] leaving DNA duplex fragments (≥12-bp) intact on the surface of the particle. These long DNA duplexes have a melting point of ≥46.4 °C, limiting target release at room temperature and thus inhibiting target recycling. These undigested fragments

and probes protect the AuNPs against salt-induced aggregation (Figure 2K), and the solution remains red (Figure 3, SM).

Successful SNP detection requires the endonucleolytic and exonucleolytic activities of Exo III to work synergistically: endonucleolytic incision distinguishes between PM and SM target sequences, whereas exonucleolytic digestion enables the target recycling process that promotes probe shearing and AuNP aggregation. To confirm that exonucleolytic digestion of Exo III is absolutely necessary to achieve aggregation of AuNPs, we performed a control experiment in which we substituted Exo III with human apurinic/apyrimidinic endonuclease 1 (APE 1). It is known that APE 1 specifically hydrolyzes the phosphodiester backbone at the 5′ end of an abasic site, creating a nick in the DNA duplex and leaving a 1-nt gapped intermediate with 3′-hydroxyl and 5′-deoxyribose phosphate termini;[29] however, this enzyme possesses no exonucleolytic activity. When we

added 100 nM APE 1, we observed that mixtures containing CP-modified AuNPs either alone or combined with the PM or SM target all remained red after 4 h (Figure 4). This indicates
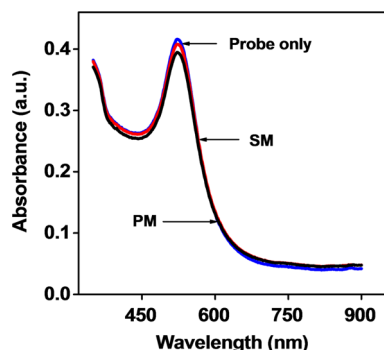

Figure 4. CP-modified AuNPs remain protected against salt-induced aggregation even after 4 h treatment with APE 1, which lacks exonuclease activity. UV−vis spectra of the modified AuNPs alone or with 20 nM PM or SM in the presence of 100 nM APE 1 are represented.

that the CP fragments remain bound to the AuNPs in the absence of 3′-to-5′ exonucleolytic activity and continue to protect the AuNPs against salt-induced aggregation.

To further confirm the contribution of this exonucleolytic activity of Exo III to AuNP-based detection, we performed Exo III- or APE 1-mediated enzymatic digestion of unmodified CP probes (**4**, 39-nt) without 5′ poly(T$_6$) ends hybridized to PM

(**5**, 41-nt) or SM (**6**, 41-nt) targets that were protected by a poly(T$_8$) 3′ end. Gel electrophoresis analysis demonstrated that both enzymes are capable of specifically discriminating a single mismatch at the SNP site (Figure 5). We were able to visualize all three main products of enzymatic cleavage (27-base, 23-base, and 16-base) with both nucleases via 12% denaturing polyacrylamide gel electrophoresis (PAGE), although in varying amounts that reflected differences in processing between different enzyme-duplex combinations (Figure 5).

When we digested with Exo III, efficient endonucleolytic incision of CP/PM at the matched 5′ abasic site yielded products of 12-nt and 27-nt, which were largely absent in the mismatch-containing CP/SM sample. The matched 3′ abasic site was efficiently incised for both duplexes, resulting in products of 16-nt and 23-nt (Figure 5A). Because Exo III is inactivated on the mismatched 5′ abasic site for the CP/SM duplex, we observed a higher enzymatic efficiency at its matched 3′ abasic site (Figure 5B, 23-nt product). Because Exo III could subsequently recognize the nicked 3′ ends and exonucleolytically digest the incised CP fragments (Figure 5A), the intact target was recycled, and most of the 39-nt probes were depleted in the PM sample and only a very small amount of 27- and 23-nt products remained after this reaction (Figure 5B, PM with Exo III). In contrast, with Exo III-treated CP/SM duplexes, the exonucleolytic activity is significantly inhibited as Exo III approaches the mismatch-flanked 5′ abasic site, inhibiting target release and thus preventing target recycling. As such, a large amount of the probe remains intact in this sample (Figure 5B, SM with Exo III). We observed a smeared band of ∼23 bases in the CP/SM samples, indicating that the
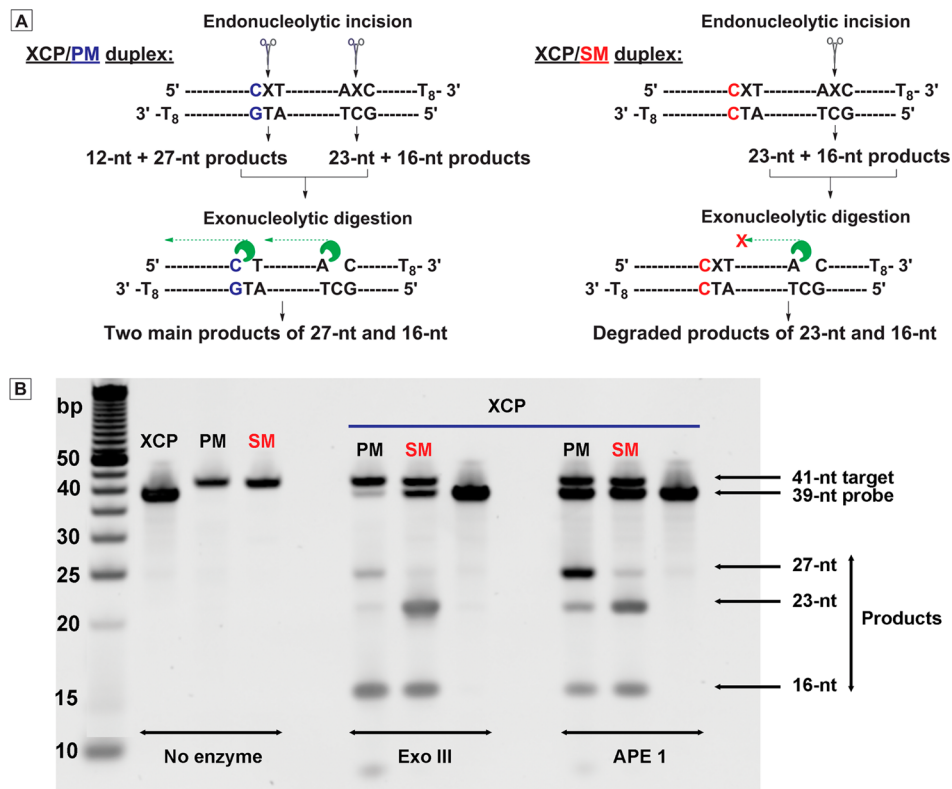

Figure 5. (A) Both Exo III and APE 1 are capable of SNP discrimination through endonucleolytic incision, although APE1 is unable to generate an amplified signal via target recycling due to the absence of exonuclease activity. (B) Gel image of unmodified CP (**4**) alone or with the poly(T$_8$)-protected PM (**5**) or SM (**6**) target (10:1 probe/target ratio), either without enzyme, or incubated with 10 units of Exo III or 100 nM APE 1. After heating at 80 °C for 10 min to stop the reaction, we characterized the samples via 12% PAGE.

initial 23-nt product is being degraded to various smaller products by Exo III exonucleolytic digestion. No exonucleolytic digestion of Exo III is occurred on the poly(T_8) related 16-nt incised product in both samples.

APE 1 also cleaves efficiently at both the 5′ and 3′ abasic sites with the PM target (Figure 5). Clearly, we observed enhanced cleavage at the matched 5′ abasic site with the PM target, producing an increased amount of the 27-nt fragment (Figure 5B, PM with APE 1). This is because the 5′ matched abasic site exhibits a higher T_m (51.5 °C) than the 3′ matched abasic site (T_m = 44.6 °C), and this increased thermal stability results in a higher concentration of formed duplexes and thus a higher endonuclease cleavage efficiency.[30] As with Exo III, APE 1 fails to cleave the mismatched 5′ abasic site in the CP/SM sample, producing only a minimal amount of 27-nt product, but yields a large quantity of 23- and 16-nt products due to efficient cleavage at the matched 3′ abasic site (Figure 5B, SM with APE 1). However, because APE 1 does not possess 3′-to-5′ exonucleolytic activity, each of these cleaved products appears as a sharp, clear band in the gel. In contrast to the Exo III-treated PM sample, most of the 39-nt probe remains unprocessed in the APE 1-treated PM sample (Figure 5B). In the absence of exonucleolytic digestion, it is most likely that each target molecule only hybridizes with a single CP molecule, with no subsequent target recycling to amplify the reaction. Because all of the nicked duplexes have a T_m well above room temperature, thermally induced dissociation of CP-target complexes is also unlikely.

These results demonstrate the critical contribution of Exo III to our assay. Exo III-assisted fragment digestion and target recycling in the PM sample result in thorough removal of CP strands from the particle surface, rendering them susceptible to salt-induced aggregation and yielding a visible color change. In contrast, although APE 1 can achieve successful SNP discrimination through selective endonucleolytic cleavage at the matched abasic site, there is no subsequent target recycling, and the remaining cleaved fragments and probes effectively protect the AuNPs against salt-induced aggregation, thereby preventing a colorimetric readout.

Both the endonuclease and exonuclease activities of Exo III are greatly affected by divalent cations.[27] To achieve optimal speed and accuracy of SNP detection, we assessed the impact of cation concentrations on Exo III activity. We achieved this by measuring the single-base mismatch discrimination factor (DF) at different concentrations of calcium and magnesium. The DF is defined as the ratio of the net colorimetric signal gain at 650 nm (after subtracting background from probe only) obtained from AuNPs with the PM target relative to that obtained with the SM target; thus, a larger DF is indicative of better specificity. Ca^{2+} is a well-known analogue for Mg^{2+} that contributes to the DNA binding specificity of Exo III for its endonuclease function.[32] Previous reports have demonstrated that in the presence of Ca^{2+}, Exo III displays only 7 ± 2% of its normal endonucleolytic activity at C—C mismatched 5′ abasic sites relative to its activity at a matched C—G pair.[27] In order to maximize SNP discrimination, we first optimized the concentration of Ca^{2+} in the system. We used buffer containing 3 mM Mg^{2+} to produce a high-efficiency Exo III reaction, with varied concentrations of Ca^{2+} ranging from 0 to 30 mM. In the absence of Ca^{2+}, we observed only modest discrimination (DF = 2) after 150 min. When we increased the Ca^{2+} concentration to 10 mM, we obtained a maximum DF of 30 after 85 min (see SI, Figure S1). As we increased the Ca^{2+}

concentration to 20 mM, we were able to achieve visible detection after 15 min—5-fold faster than the reaction with 10 mM Ca^{2+}, presumably because the elevated concentration of Ca^{2+} enhanced the salt-induced aggregation of AuNPs. Although the presence of Ca^{2+} enhances formation of the protein—metal—DNA complex, these ions can also inhibit the enzyme's endonucleolytic activity.[32] Accordingly, at Ca^{2+} concentrations of 20 mM or higher, the DF decreased to 12 (SI, Figure S1).

Mg^{2+} strongly stimulates the 3′ to 5′ exonuclease activity of Exo III due to its suitable ionic radius and electronegativity,[33] and we sought to further optimize assay performance by adjusting the concentration of Mg^{2+}. We fixed the buffer Ca^{2+} concentration at 20 mM and varied the Mg^{2+} concentration between 0 and 10 mM. We found that the activities of Exo III increased as we raised the Mg^{2+} concentration, achieving a maximum DF of 14 with 2 mM Mg^{2+} after 40 min (SI, Figure S2). At higher Mg^{2+} concentrations, the reaction rate accelerated but the DF decreased due to nonspecific digestion of CP/SM duplexes by Exo III; thus, we observed that the DF decreased to a plateau of 10 at Mg^{2+} concentrations ≥4 mM. In order to balance reaction speed and specificity, we selected a reaction buffer containing 3 mM Mg^{2+} and 20 mM Ca^{2+}. This formulation ensures that Exo III efficiently binds and cleaves at matched abasic sites and performs rapid exonucleolytic digestion of the resulting fragments while also inhibiting Exo III binding of mismatched abasic site, yielding good specificity (with a DF of 12) within 15 min. Under these reaction conditions, our assay allows us to detect as little as 10 nM PM target at room temperature after 15 min by naked eye (SI, Figure S3). In contrast, the sensor generated only a slight signal change with SM target during the first 2 h. We can greatly improve the sensitivity of the AuNP-based/Exo-amplified SNP assay at lower temperatures, although there is a trade-off between reaction time and limit of detection. We obtained a detection limit of 2 nM ($S/N > 3$) by performing the reaction at 4 °C for 4 h, and the color change was great enough for naked eye observation (SI, Figure S4). This may be slow, but it has the advantage of being significantly simpler than other reported SNP assays and competes well in terms of specificity and sensitivity.

Because the hybridization between the AuNP-attached CP probe and DNA target is relatively rapid in homogeneous solution,[34] we presume that exonuclease digestion-mediated AuNP aggregation is the rate-limiting step. We assume that the AuNPs are only able to aggregate when all or a great majority of the CP probes are sheared from the particle. We performed a time course of reactions between CP-modified AuNPs and both PM (2) or SM (3) and estimated the rate constants of the enzymatic reaction by fitting the time course data to the Michaelis—Menten equation (Figure 6). For the PM sample, we calculated a Michaelis—Menten constant (K_m) of 426 ± 20 nM, an apparent turnover number for target DNA (k_{cat}) of 1.26 min^{-1}, and thus a reaction efficiency (k_{cat}/K_m) for Exo III of 0.0030 min^{-1} nM^{-1}. In contrast, we could not obtain accurate calculation of rate constants for the SM reaction due to the much slower Exo III reaction. Our K_m value for the AuNP-attached CP system is ~3 times lower than that of Exo III observed in solution,[27] suggesting that the k_{cat} in our SNP sensor incorporates the rate constraints for incision and digestion of Exo III and the aggregation of AuNPs.

Lastly, we demonstrated the generality of our SNP sensor by testing its discrimination ability against SM targets containing
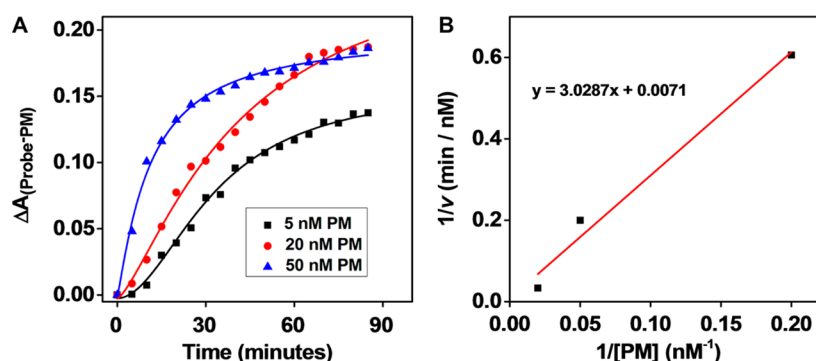
Figure 6. Determination of Exo III kinetics in the AuNP-attached CP system. (A) Time course of our SNP sensor at different PM target concentrations. The absorbance difference (ΔA) between AuNP-attached probe alone and with PM was recorded at 524 nm. (B) We calculated the rate constant of the Exo III reaction by fitting time-course data to the Michaelis−Menten equation.
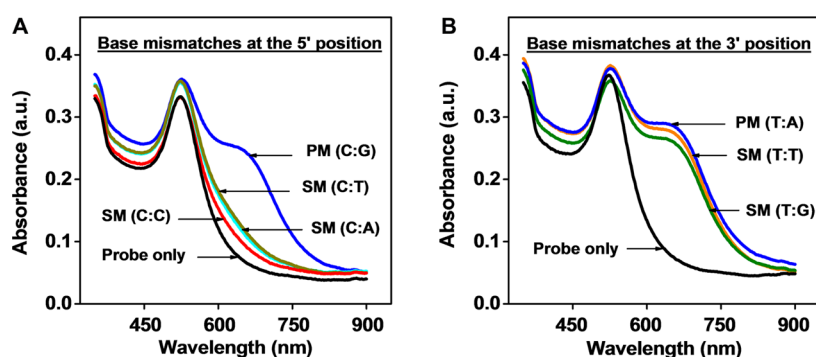

Figure 7. Generality of mismatch detection of the AuNP-based, Exo III-amplified sensor. (A) Our sensor can effectively discriminate SM from PM regardless of which mismatched base is located at the 5′ abasic site. (B) In contrast, our sensor could not discriminate mismatches positioned 3′ to the 5′ abasic site, due to the 5′ endonucleolytic activity of Exo III. Data show UV−vis spectra of CP-modified AuNPs probe alone or with 20 nM PM or SM sequences after a 15 min incubation with Exo III at room temperature.

different single-base mismatches (C−C (**3**), C−T (**7**), and C−A (**8**)) at the 5′ abasic site. The current sensor offers highly accurate SNP detection, and we can easily detect any single-base mismatch (C, T, or A) located within a 33-nt DNA strand. We found that assays with SM targets containing all three mismatched bases remained red after 2 h, whereas the PM target generated a blue color switch after 15 min (Figure 7A). The highest level of discrimination occurred with duplexes containing a C−C mismatch (DF = 12), whereas the lowest level was observed with a C−T mismatch (DF = 8.5). This variability is to be expected, because mismatch thermodynamics depend on the identity of the mismatched base pair as well as the identity of its near neighbors.[35] On the other hand, these results are in contrast to a report by Masayoshi et al. that the endonucleolytic activity of Exo III is only meaningfully inhibited by a C−C mismatch positioned 5′ to an abasic site.[27] When we switched the single-base mismatches (T−T (**9**) and T−G (**10**)) from the 5′ to the 3′ side of the 5′ abasic site, we no longer observed the ability to discriminate single-base mismatches (Figure 7B), confirming that Exo III-mediated SNP discrimination is based on its 5′ endonucleolytic activity.[36]

We report here a remarkably simple platform that enables sensitive, naked-eye detection of SNPs at room temperature within 15 min. The entire assay is performed in a single tube with one set of DNA probe-modified AuNPs, a single enzyme, and the target DNA. In the presence of a perfectly matched target, target−probe duplexes are first endonucleolytically cleaved by Exo III at both matched abasic sites on the probe to form nicked duplexes, and the nicked strands are then rapidly degraded via the exonucleolytic action of Exo III, thus releasing the target. The released target can then hybridize with another probe to start the cycle anew. This recycling process amplifies the signal from the PM target and ultimately strips the probes from the AuNPs, resulting in salt-induced AuNP aggregation with a visible color change to blue as a readout. In contrast, the initial endonucleolytic processing is inhibited for mismatched targets, stalling exonucleolytic digestion, and the AuNP solution remains red in color. This color change is easily observed with as little as 2 nM target by naked eye, which is 100 times lower than the target concentration that is required for reliable naked eye observation with unmodified AuNPs in well-optimized reaction conditions.[23] However, a 2 nM detection limit will not be sufficient to omit a target amplification step. To obtain clinically relevant sensitivity (∼ fM), we are now working to incorporate an amplification strategy into this SNP detection platform to achieve real-time SNP detection at low pM or fM concentrations. Because the aggregation of AuNPs is caused by Exo III-mediated DNA shearing from the particle surface, we expect that this system could also be rendered applicable in complex biological samples by using nuclease-resistant phosphorothioated probes.

Importantly, our SNP detection system can readily discriminate SNP-containing targets regardless of which mismatched base is positioned at the 5′ abasic site. This feature provides direct SNP detection without the need of complicated probe design. No specialized equipment is required because SNP is colorimetrically dicriminated in one-step, one-pot reaction at room temperature. Those attributes offer the opportunity

for multitarget, parallel SNP analysis over molecule beacons[37] and TaqMan probes,[38] which often require delicate probe design and precise temperature control. Our colorimetric detection platform can be easily transferred into a multiplexed, paper-based device to permit rapid, cheap, and immediate screening of SNPs. Given that a short abasic site inserted oligonucleotide could be introduced to hybridize the target-binding portion of any aptamer,[39] we believe that our platform can be generalized for the detection of a variety of non-DNA targets, including proteins, small molecules, metal ions, and even whole cells.

■ ASSOCIATED CONTENT

ⓢ Supporting Information

AuNP synthesis, modification of AuNPs with thiolated CP probe, colorimetric detection of DNA, polyacrylamide gel electrophoresis, the influence of Ca^{2+} or Mg^{2+} concentration on target discrimination and detection time, the dynamic range and detection limit of our AuNP-based, Exo III-amplified sensor. This material is available free of charge via the Internet at http://pubs.acs.org.

■ AUTHOR INFORMATION

Corresponding Author

*E-mail: yxiao2@fiu.edu.

Notes

The authors declare no competing financial interest.

■ ACKNOWLEDGMENTS

■ REFERENCES

(1) Wang, D. G.; Fan, J. B.; Siao, C. J.; Berno, A.; Young, P.; Sapolsky, R.; Ghandour, G.; Perkins, N.; Winchester, E.; Spencer, J.; Kruglyak, L.; Stein, L.; Hsie, L.; Topaloglou, T.; Hubbell, E.; Robinson, E.; Mittmann, M.; Morris, M. S.; Shen, N.; Kilburn, D.; Rioux, J.; Nusbaum, C.; Rozen, S.; Hudson, T. J.; Lipshutz, R.; Chee, M.; Lander, E. S. *Science* **1998**, *280*, 1077−1082.

(2) Lai, E. *Genome Res.* **2001**, *11*, 927−929.

(3) Chakravarti, A. *Nature* **2001**, *409*, 822−823.

(4) Kurg, A.; Tõnisson, N.; Georgiou, I.; Shumaker, J.; Tollett, J.; Metspalu, A. *Genet. Test.* **2000**, *4*, 1−7.

(5) Matsuzaki, H.; Dong, S.; Loi, H.; Di, X.; Liu, G.; Hubbell, E.; Law, J.; Berntsen, T.; Chadha, M.; Hui, H.; Yang, G.; Kennedy, G. C.; Webster, T. A.; Cawley, S.; Walsh, P. S.; Jones, K. W.; Fodor, S. P. A.; Mei, R. *Nat. Methods* **2004**, *1*, 109−111.

(6) Kuppuswamy, M. N.; Hoffmann, J. W.; Kasper, C. K.; Spitzer, S. G.; Groce, S. L.; Bajaj, S. P. *Proc. Natl. Acad. Sci. U.S.A.* **1991**, *88*, 1143−1147.

(7) Landegren, U.; Kaiser, R.; Sanders, J.; Hood, L. *Science* **1988**, *241*, 1077−1080.

(8) Lyamichev, V.; Mast, A. L.; Hall, J. G.; Prudent, J. R.; Kaiser, M. W.; Takova, T.; Kwiatkowski, R. W.; Sander, T. J.; de Arruda, M.; Arco, D. A.; Neri, B. P.; Brow, M. A. D. *Nat. Biotechnol.* **1999**, *17*, 292−296.

(9) Lee, L. G.; Connell, C. R.; Bloch, W. *Nucleic Acids Res.* **1993**, *21*, 3761−3766.

(10) Howell, W. M.; Jobs, M.; Gyllensten, U.; Brookes, A. J. *Nat. Biotechnol.* **1999**, *17*, 87−88.

(11) Tyagi, S.; Bratu, D. P.; Kramer, F. R. *Nat. Biotechnol.* **1998**, *16*, 49−53.

(12) (a) Kolpashchikov, D. M. *J. Am. Chem. Soc.* **2005**, *127*, 12442−12443. (b) Kolpashchikov, D. M. *J. Am. Chem. Soc.* **2006**, *128*, 10625−10628.

(13) Xiao, Y.; Plakos, K. J. I.; Lou, X. H.; White, R. J.; Qian, J. R.; Plaxco, K. W.; Soh, H. T. *Angew. Chem., Int. Ed.* **2009**, *121*, 4418−4422.

(14) Jans, H.; Huo, Q. *Chem. Soc. Rev.* **2012**, *41*, 2849−2866.

(15) Mout, R.; Moyano, D. F.; Rana, S.; Rotello, V. M. *Chem. Soc. Rev.* **2012**, *41*, 2539−2544.

(16) Stewart, M.; Anderton, C. R.; Thompson, L. B.; Maria, J.; Gray, S. K.; Rogers, J. A.; Nuzzo, R. G. *Chem. Rev.* **2008**, *108*, 494−521.

(17) Elghanian, R.; Storhoff, J. J.; Mucic, R. C.; Letsinger, R. L.; Mirkin, C. A. *Science* **1997**, *277*, 1078−1081.

(18) Li, H. X.; Rothberg, L. J. *J. Am. Chem. Soc.* **2004**, *126*, 10958−10961.

(19) Xu, W.; Xue, X. J.; Li, T. H.; Zeng, H. Q.; Liu, X. G. *Angew. Chem., Int. Ed.* **2009**, *48*, 6849−6852.

(20) Li, J. S.; Deng, T.; Chu, X.; Yang, R. H.; Jiang, J. H.; Shen, G. L.; Yu, R. Q. *Anal. Chem.* **2010**, *82*, 2811−2816.

(21) Shen, W.; Deng, H. M.; Gao, Z. Q. *J. Am. Chem. Soc.* **2012**, *134*, 14678−14681.

(22) Li, H. X.; Rothberg, L. *Proc. Natl. Acad. Sci. U.S.A.* **2004**, *101*, 14036−14039.

(23) Sato, K.; Hosokawa, K.; Maeda, M. *Nucleic Acids Res.* **2005**, *33*, e4.

(24) Shida, T.; Noda, M.; Sekiguchi, J. *Nucleic Acids Res.* **1996**, *24*, 4572−4576.

(25) Turkevich, J.; Stevenson, P. C.; Hillier, J. *Discuss. Faraday Soc.* **1951**, *11*, 55−75.

(26) Henikoff, S. *Gene* **1984**, *28*, 351−359.

(27) Takeuchi, M.; Lillis, R.; Demple, B.; Takeshita, M. *J. Biol. Chem.* **1994**, *269*, 21907−21914.

(28) Zhang, L. K.; Rempel, D.; Gross, M. L. *Anal. Chem.* **2001**, *73*, 3263−3273.

(29) Wilson, D. M., III *J. Mol. Biol.* **2005**, *345*, 1003−1014.

(30) Sági, J.; Hang, B.; Singer, B. *Chem. Res. Toxicol.* **1999**, *12*, 917−923.

(31) Lebedeva, N. A.; Khodyreva, S. N.; Favre, A.; Lavrik, O. I. *Biochem. Biophys. Res. Commun.* **2003**, *300*, 182−187.

(32) Bellamy, S. R. W.; Kovacheva, Y. S.; Zulkipli, I. H.; Halford, S. E. *Nucleic Acids Res.* **2009**, *37*, 5443−5453.

(33) Erzberger, J. P.; Wilson, D. M., III *J. Mol. Biol.* **1999**, *290*, 447−457.

(34) Pei, H.; Lu, N.; Wen, Y. L.; Song, S. P.; Liu, Y.; Yan, H.; Fan, C. H. *Adv. Mater.* **2010**, *22*, 4754−4758.

(35) Fish, D. J.; Horne, M. T.; Brewood, G. P.; Goodarzi, J. P.; Alemayehu, S.; Bhandiwad, A.; Searles, R. P.; Benight, A. S. *Nucleic Acids Res.* **2007**, *35*, 7197−7208.

(36) Kow, Y. W. *Biochemistry* **1989**, *28*, 3280−3287.

(37) Dubertret, B.; Calame, M.; Libchaber, A. J. *Nat. Biotechnol.* **2001**, *19*, 365−370.

(38) Heid, C. A.; Stevens, J.; Livak, K. J.; Williams, P. M. *Genome Res.* **1996**, *6*, 986−994.

(39) Bock, L. C.; Griffin, L. C.; Latham, J. A.; Vermaas, E. H.; Toole, J. J. *Nature* **1992**, *355*, 564−566.

3467

dx.doi.org/10.1021/ac4040373 | *Anal. Chem.* 2014, 86, 3461−3467